


Discovery of a third body around semi-detached binary V527 Dra through eclipse timing and radial velocity variations

H.V. Şenavcı^{1,2} , D. Bohlender³, E. Bahar^{1,2}, S. Gu⁴, İ. Özavcı^{1,2},
M. Yılmaz^{1,2}, E.B. Yorulmaz^{1,2}, O. Latković⁵ and A. Čeki⁵

¹ *Ankara University, Faculty of Science, Astronomy & Space Sciences
Department, Tandoğan, TR-06100, Ankara, Türkiye
(E-mail: hvsenavci@ankara.edu.tr)*

² *Ankara University, Astronomy and Space Sciences Research and Application
Center (Kreiken Observatory), İncek Blvd., TR-06837, Ahlatlıbel, Ankara,
Türkiye*

³ *Canadian Astronomy Data Centre & Dominion Astrophysical Observatory,
Herzberg Astronomy and Astrophysics Research Centre, National Research
Council of Canada 5071 West Saanich Road, Victoria, BC V9E 2E7,
Canada*

⁴ *Yunnan Observatories, Chinese Academy of Sciences, Kunming 650216,
People's Republic of China*

⁵ *Astronomical Observatory, Volgina 7, 11000 Belgrade, Serbia*

Received: October 2, 2024; Accepted: January 2, 2025

Abstract. The mid-eclipse times obtained using TESS data for the semi-detached binary V527 Dra show cyclic variations attributed to the presence of an additional body. Additionally, the broadening profiles (BFs) of V527 Dra, obtained from spectroscopic data gathered between 2020 and 2024, reveal a third peak with varying radial velocities over time, further indicating the presence of a third body. Therefore, in this study, using the radial velocity variations of the third component and the eclipse timing variations from the TESS data, we were able to constrain the orbital parameters of the third component.

Key words: Stars: individual: V527 Dra – (Stars:) binaries (including multiple): close – Techniques: radial velocities

1. Introduction & motivation

For eclipsing binaries, the continuous and high-precision observations gathered using space telescopes provide valuable insights into long-term phenomena like magnetic activity and hierarchical multiple star systems, often identified through eclipse timing variations (ETV) (see [Kirk et al., 2016](#); [Prša et al., 2022](#)).

In a recent study by Čeki *et al.* (2024), we conducted a comprehensive analysis of the semi-detached eclipsing binary V527 Dra, utilizing both ground and space-based photometric data, as well as radial velocity measurements (see Čeki *et al.*, 2024, for details). During the determination of radial velocities using the broadening function (BF) technique (Rucinski, 1999, 2002, 2004), we realized the presence of third peaks in the BFs, in addition to the broadening profiles of both components of V527 Dra. Furthermore, those peaks have different velocities in the 2020 and 2021 data as seen from Figure 1.

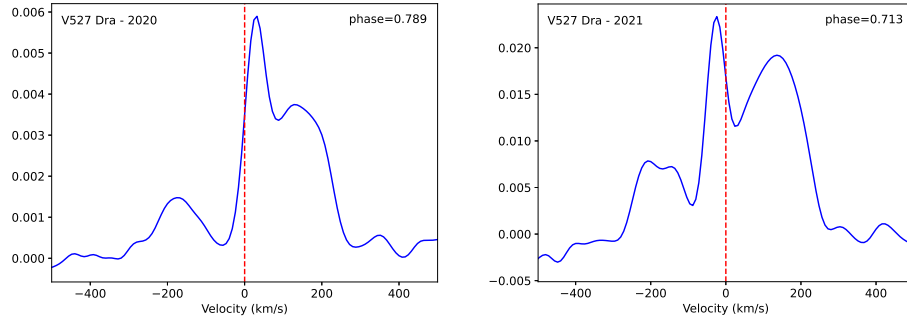


Figure 1. Example BFs of V527 Dra from 2020 and 2021 dataset. The red dashed lines show the velocity of 0 km s^{-1} . Figures are taken from Čeki *et al.* (2024).

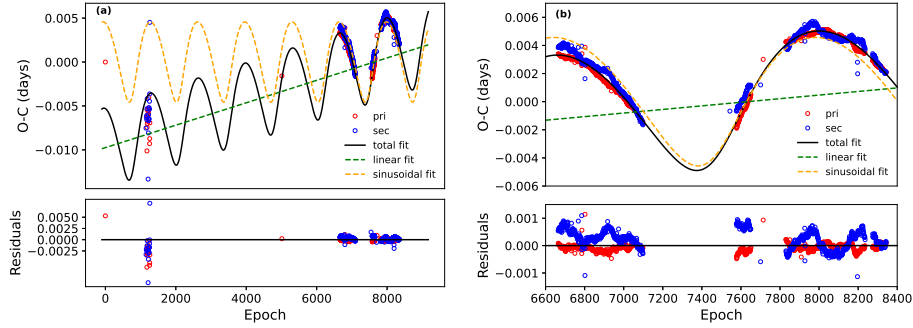


Figure 2. (a) The complete ETV diagram of V527 Dra, constructed using all available eclipse times, along with model fits incorporating the light-time effect (LiTE) and a linear trend. (b) A zoomed-in view focusing solely on the TESS data. Residuals are displayed below each plot. Figures are taken from Čeki *et al.* (2024).

In the same study by Čeki *et al.* (2024), we also investigated the eclipse timing variations (ETV) of V527 Dra, where the most of the mid eclipse times

were calculated from the TESS data. The overall ETV of the system exhibits a cyclic variation superimposed on a linear trend (see Figure 2). Under the Light-Time-Effect (LiTE) approximation and using the equations from Irwin (1952), the best-fitting LiTE model yielded a third body with a mass of $M_3 = 0.999 \pm 0.031 M_\odot$ and with a period of $P_3 = 2.733 \pm 0.005$ yr, assuming that the third body's orbit is co-planar with the binary orbit. We explored whether an additional body with a mass of $0.999 M_\odot$, as obtained from the ETV analysis, could be responsible for the observed third peak in the BFs of V527 Dra, which is the motivation of this study. A similar investigation already was conducted by our working group (see Čeki et al., 2024, for details) using two spectral dataset from 2020 and 2021, revealing that the RVs of the third peak are in fair agreement with the RV variation generated using the parameters obtained from the ETV analysis. In this study, we reinforce this agreement with the additional spectral data of the system.

2. New spectroscopic observations and RV determination

To investigate further whether this additional contribution originates from a physically bound component to the V527 Dra binary, we collected more spectroscopic data of the system at the Lijiang Observatory and the Dominion Astrophysical Observatory (DAO). The spectroscopic observations at the Lijiang Observatory were conducted using the YFOSC instrument mounted on the 2.4m Lijiang Telescope, with the resolution of $R \sim 10000$ and an exposure time of 450 seconds on April 21st. The remaining spectroscopic data were obtained using the Cassegrain spectrograph attached to the 1.83 m Plaskett Telescope, offering a resolution of $R \sim 15000$ and an exposure time of 1800 seconds during the May - September observing season. HD 184499 (G0V) was also observed as the RV standard throughout the entire observing run. The data reduction was performed using the standard IRAF packages. Radial velocity measurements were obtained by fitting a sum of Gaussian profiles to the observed peaks in the BFs, specifically using a sum of three Gaussians. The optimal values for each Gaussian profile's parameters, including amplitude, width, and peak center, were determined through an optimization process. Two examples of fitted Gaussian profiles are shown in Figure 3.

3. Results and Discussion

Using Eqn. 1, we first determined the radial velocity variation of the additional body using the parameters obtained from the ETV analysis (see Čeki et al., 2024, for details), within the timespan covering the entire dataset. Figure 4 shows the radial velocities calculated from all observations, along with the radial velocity variation for the additional body (red dashed line). The results clearly

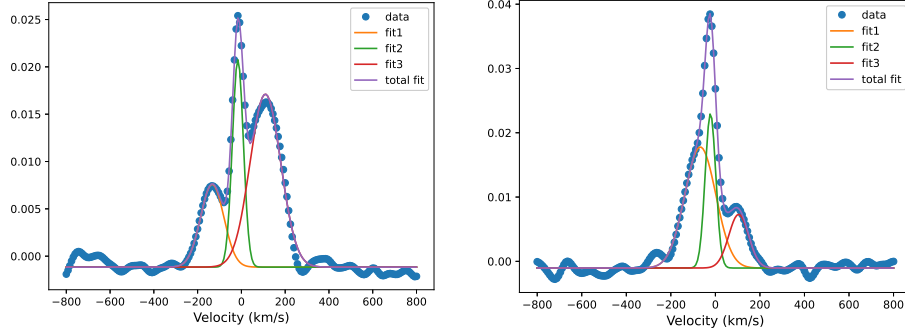


Figure 3. Two examples of Three-Gaussian profile fitting via an optimization process to the observed peaks in the BFs to determine the RVs of the components of V527 Dra.

indicate that the observed RV of the third component aligns well with the theoretical RV variation derived from the ETV analysis.

$$V_{rad} = \frac{2\pi a_3 \sin i_3}{P(1-e^2)^{1/2}} [\cos(\nu + \omega_3) + e \cos \omega_3] + V_{\gamma_3} \quad (1)$$

The radial velocity variation of the additional component (Eqn. 1) allows us to constrain $a_3 \sin i_3$ and V_{γ_3} parameters. In addition, since we determined $a_{12} \sin i_3$ and mass function $f(M_3)$ from the ETV analysis, and $M_{1,2}$ from the light and radial velocity curve analyses (Çeki *et al.*, 2024), we were able to constrain M_3 and the orbital inclination of the third body i_3 using the equations below through an optimization process:

$$\frac{a_{12} \sin i_3}{a_3 \sin i_3} = \frac{M_3}{M_1 + M_2}, f(M_3) = \frac{(M_3 \sin i_3)^3}{(M_1 + M_2 + M_3)^2} \quad (2)$$

Consequently the best-fitting RV variation, which is plotted as blue solid line in Figure 4, yielded the parameters $a_3 \sin i_3 = 1.875 \pm 0.222 AU$, $M_3 = 1.18 \pm 0.11 M_\odot$, $i_3 = 60.1 \pm 2.0^\circ$ and $V_{\gamma_3} = -0.867 \pm 0.017 \text{ km/s}$.

From the simultaneous TESS, SDSS g' , r' and i' light and velocity curve analysis of the system, Çeki *et al.* (2024) estimated the average third light contribution as $\ell_{3\text{avg}} = 0.337$. To calculate the amount of third light of the additional body with the mass of $M_3 = 1.18 M_\odot$ that we obtained from the RV variation, we used the mass-luminosity ($1.15 M^{3.36}$) and mass-radius ($\log R = 0.026 + 0.945 \log M$) relations given by Demircan & Kahraman (1991) and calculated the luminosity and the radius of the tertiary component to be $L_3 = 2.01 L_\odot$ and $R_3 = 1.24 R_\odot$, respectively. The third light is defined in terms of total flux in the given passband at maximum light as $\ell_3 = F_3 / (F_1 + F_2 + F_3)$ and the luminosity $L = 4\pi R^2 F$, where R is the radius of star and F is the bolometric

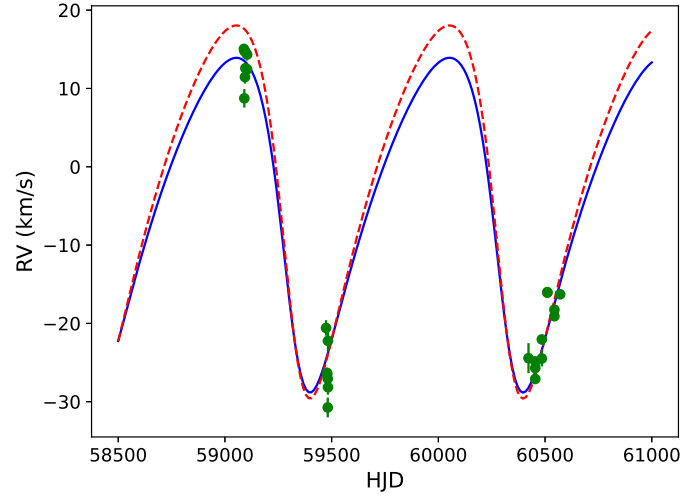


Figure 4. RV variation of the third body, of which the parameters were calculated from the ETV analysis, assuming a coplanar orbit with the binary system (red dashed lines). Green dots represent radial velocities of the third body derived from BFs. The blue solid line shows the RV variation of the third body after adjusting $asini_3$ of the third body and systemic velocity of the triple system.

flux. Neglecting the difference between bolometric and passband-specific flux as well as the limb darkening and the gravity darkening, we could roughly obtain the third light (ℓ_3) via Eqn. 3 given below:

$$\ell_3 = \frac{L_3/R_3^2}{L_1/R_1^2 + L_2/R_2^2 + L_3/R_3^2} \quad (3)$$

The resulting light contribution of the tertiary component is $\ell_3 = 0.299$, which is quite consistent with the value obtained through the light curve analysis by Čeki et al. (2024).

Observing the radial velocity of the additional component combined with the parameters obtained from the ETV analysis offers a unique opportunity to determine the orbital parameters and the mass of the additional component more accurately. With further spectroscopic observations of V527 Dra, the orbital parameters of the additional body can be determined with greater precision, and the systemic velocity of the binary can be measured to confirm the physical connection.

Acknowledgements. Based on observations obtained at the Dominion Astrophysical Observatory, Herzberg Astronomy and Astrophysics Research Centre, National Research Council of Canada.

References

- Demircan, O. & Kahraman, G., Stellar Mass / Luminosity and Mass / Radius Relations. 1991, *Astrophysics and Space Science*, **181**, 313, DOI:10.1007/BF00639097
- Irwin, J. B., The Determination of a Light-Time Orbit. 1952, *ApJ*, **116**, 211, DOI:10.1086/145604
- Kirk, B., Conroy, K., Prša, A., et al., Kepler Eclipsing Binary Stars. VII. The Catalog of Eclipsing Binaries Found in the Entire Kepler Data Set. 2016, *Astronomical Journal*, **151**, 68, DOI:10.3847/0004-6256/151/3/68
- Prša, A., Kochoska, A., Conroy, K. E., et al., TESS Eclipsing Binary Stars. I. Short-cadence Observations of 4584 Eclipsing Binaries in Sectors 1-26. 2022, *Astrophysical Journal, Supplement*, **258**, 16, DOI:10.3847/1538-4365/ac324a
- Rucinski, S., Determination of Broadening Functions Using the Singular-Value Decomposition (SVD) Technique. 1999, in *Astronomical Society of the Pacific Conference Series*, Vol. **185**, *IAU Colloq. 170: Precise Stellar Radial Velocities*, ed. J. B. Hearnshaw & C. D. Scarfe, 82
- Rucinski, S. M., Radial Velocity Studies of Close Binary Stars. VII. Methods and Uncertainties. 2002, *Astronomical Journal*, **124**, 1746, DOI:10.1086/342342
- Rucinski, S. M., Advantages of the Broadening Function (BF) over the Cross-Correlation Function (CCF). 2004, in *American Astronomical Society Meeting Abstracts*, Vol. **215**, *Stellar Rotation*, ed. A. Maeder & P. Eenens, 17
- Čeki, A., Şenavcı, H. V., Latković, O., et al., Comprehensive analysis of the eclipsing binaries V527 Dra and V2846 Cyg. 2024, *Monthly Notices of the RAS*, **532**, 3582, DOI:10.1093/mnras/stae1709